The Effect of Pad-asperity Curvature on Material Removal Rate in Chemical-mechanical Polishing

Available online at www.sciencedirect.com

ScienceDirect

Procedia CIRP 14 (2014) 42 – 47

www.elsevier.com/locate/procedia

6th CIRP International Conference on High Performance Cutting, HPC2014

The Effect of Pad-Asperity Curvature on Material Removal Rate in Chemical-Mechanical Polishing

Sanha Kim[a,*], Nannaji Saka[a], Jung-Hoon Chun[a]

[a]*Laboratory for Manufacturing and Productivity, Massachusetts Institute of Technology, 77 Massachusetts Ave., Cambridge, MA 02139, USA*

* Corresponding author. Tel.: +1-617-715-4783; fax: +1-617-253-1556. *E-mail address:* sanhkim@mit.edu

Abstract

In chemical-mechanical polishing (CMP), surface asperities of the polishing pad play a key role, for they transmit normal force and impart tangential motion to the hard, nano-scale abrasive particles in the slurry. It has been shown recently, however, that the soft pad asperities themselves often generate micro-scale scratches on the surfaces being polished. To mitigate scratching by pad asperities, therefore, topography control by flattening pad asperities has been proposed and experimentally validated. In this study, the effects of asperity-flattening on pad topography and the material removal rate are investigated. It is found both theoretically and experimentally that even at a relatively high pressures only the tallest of the asperities are flattened and the ratio of asperity radius-to-standard deviation of heights is increased, but the average roughness itself is little affected. Specifically, surface profiles of new and asperity-flattened pads indeed show that the average roughness of about 5 μm is changed less than ten percent. Concurrently, the material removal rate is increased by about 30 percent due in part to the increased real area of contact—the result of increased asperity radius of curvature and decreased standard deviation of asperity heights.

Selection and peer-review under responsibility of the International Scientific Committee of the 6th CIRP International Conference on High Performance Cutting

Keywords: Polishing; Defect; Semiconductor

1. Introduction

Over the decades, the semiconductor industry has responded to the ever-increasing demand for high-performance ultra-large-scale integrated (ULSI) electronics by designing and fabricating submicron features of finer resolution, denser packing, and multi-level structures. In this relentless endeavor for meeting the ever-stringent specifications, the Chemical-Mechanical Planarization or Polishing (CMP) process has played a vital role due to its global and local planarization capabilities. The CMP process is now ubiquitous in many stages of the manufacture of ULSI circuits [1].

One of the primary focuses in CMP is the material removal rate (MRR). A phenomenological model for MRR in glass polishing was proposed by Preston as early as in 1927 [2]. It was empirically found that the rate of thickness change, dh/dt, is directly proportional to the applied nominal pressure, p, and the relative velocity, v_r, as

$$\frac{dh}{dt} = k_p p v_r \tag{1}$$

where k_p is a constant, now designated Preston constant. This equation represents the minimum number of variables required to describe the CMP process. Although the above relation has been experimentally validated adequately, the effects of several process variables are not explicit and are hidden in k_p. Several papers have been published recently to elucidate the role of the other process parameters on MRR [3-5].

As demands on metal interconnects and surface structures are becoming ever-stringent, however, micro- and nano- scale scratching has lately emerged as a critical problem in integrated circuit (IC) manufacturing due both to the shrinkage of the feature size and to the prevalence of low-k dielectrics [6,7]. During the polishing process, scratches may

Selection and peer-review under responsibility of the International Scientific Committee of the 6th CIRP International Conference on High Performance Cutting
doi:10.1016/j.procir.2014.03.014

be generated either by abnormally large particles, due to agglomeration, or by pad-asperities, due to the height variation and high friction [8,9]. To optimize the CMP process, therefore, not only the improvement of MRR but also the mitigation of scratching must be addressed.

Recently, pad topography control by asperity-flattening has been introduced as a cost-effective method for mitigating pad scratching in CMP [10,11]. Contact mechanics models and scratching experiments have shown that pad scratching can be minimized by flattening the asperities, i.e., by increasing the radius of tall asperities and reducing their height variation. Topographical changes may also affect MRR, for topography plays a key role in material removal. The preliminary polishing experiments with topography-controlled pads have shown that MRR increases as the asperities are flattened [10].

The objective of this study, accordingly, is to investigate the effects of asperity-flattening on pad topography and on MRR. First, explicit equations for real contact area between a rough pad and a flat wafer are presented based on multi-asperity contact models. Then, the surface roughness, asperity radius and standard deviation of asperity heights of asperity-flattened pads are determined and used to predict the contact area ratio. Finally, the MRR results of polishing experiments employing the topography-controlled pads are compared with the theoretical predictions.

Nomenclature

A_a	asperity contact area [m^2]
A_n	nominal contact area [m^2]
A_r	real contact area [m^2]
d	separation distance [m]
k_p	Preston constant [N^{-1} m^2]
E_a	Young's modulus of pad asperity [N m^{-2}]
H_a	hardness of pad asperity [N m^{-2}]
h	surface layer thickness [m]
p	applied pressure [N m^{-2}]
p_a	applied pressure at an asperity [N m^{-2}]
R_a	asperity radius [m]
t	process time [s]
V	volume of surface layer removed by particles [m^3]
v_r	relative velocity [m s^{-1}]
z_a	asperity height [m]
δ	approach of distant points [m]
δ_y	approach of distant points at the onset of asperity yielding [m]
$\delta_{f\text{-}p}$	approach of distant points at the onset of fully-plastic deformation [m]
λ_p	particle spacing [m]
ξ	$= (z_a - d) / \sigma_z$
$\sigma_{y,a}$	yield strength of asperity [N m^{-2}]
σ_z	standard deviation of asperity heights [m]
ψ	plasticity index
$\phi(z_a)$	probability density of asperity height [m^{-1}]

2. Contact area ratio and material removal rate

To elucidate the material removal and scratching mechanisms in CMP, interaction between the pad and the wafer should be examined at different scales: macro-, micro- and nano- scales, Fig. 1. The surface layer, oxidized by slurry chemicals, is polished primarily by the nano-sized particles entrapped at the pad asperity contacts, Fig. 1c. From the microscopic point of view, however, only a small fraction of the pad surface will be in contact with the wafer due to the relatively large roughness of polishing pads, Fig. 1b. The polishing rate, accordingly, strongly depends on the ratio of real contact area to the nominal contact area, which generally is less than a percent.

Assuming that particle spacing, λ_p, and removal rate by each particle, $(dV/dt)_p$, are uniform everywhere in the asperity contact, the wear rate of the surface layer, dh/dt, can be written as [4,5]:

$$\frac{dh}{dt} = \frac{N_{active}}{A_n}\left(\frac{dV}{dt}\right)_p = \frac{1}{\lambda_p^2}\left(\frac{dV}{dt}\right)_p \cdot \frac{A_r}{A_n} \tag{2}$$

Thus the material removal rate will be proportional to the ratio of the real and nominal contact areas, A_r/A_n [12].

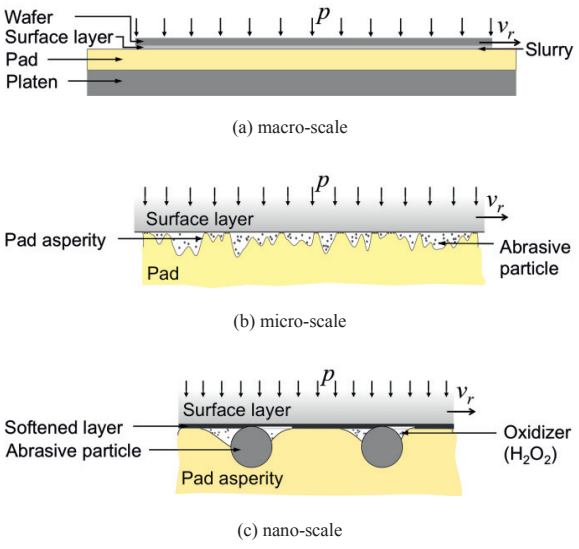

Fig. 1. Schematic of the contact between a rough pad and a smooth wafer.

When an asperity is pressed against a smooth flat surface, it experiences mainly three distinct deformation modes as the approach of distant points, δ, increases: elastic ($0 \le \delta \le \delta_y$), elastic-plastic ($\delta_y \le \delta \le \delta_{f\text{-}p}$), and fully-plastic ($\delta_{f\text{-}p} \le \delta$). For a homogeneous and isotropic material with Young's modulus, E_a, yield strength, $\sigma_{y,a}$, and hardness, H_a, the contact area and pressure at an asperity with radius R_a can be expressed as a function of δ as [13,14]:

$$A_a(\delta)=\begin{cases}\pi R_a\delta & \text{if } 0\le\delta\le\delta_y\\ \pi R_a\delta\left[1+3\left(\frac{\delta/\delta_y-1}{53}\right)^2-2\left(\frac{\delta/\delta_y-1}{53}\right)^3\right] & \text{if } \delta_y\le\delta\le\delta_{f\text{-}p}\\ 2\pi R_a\delta & \text{if } \delta_{f\text{-}p}\le\delta\end{cases} \quad (3)$$

$$p_a(\delta)=\begin{cases}\frac{4}{3\pi}E_a\left(\frac{\delta}{R_a}\right)^{1/2} & \text{if } 0\le\delta\le\delta_y\\ \sigma_{y,a}\left[1+\frac{1}{2}\ln\left(\delta/\delta_y\right)\right] & \text{if } \delta_y\le\delta\le\delta_{f\text{-}p}\\ H_a & \text{if } \delta_{f\text{-}p}\le\delta\end{cases} \quad (4)$$

where δ_y can be estimated by [15]

$$\delta_y=\frac{9\pi^2}{16}\frac{\sigma_y^2}{E_a^2}R_a\cong\frac{\pi^2}{16}\frac{H_a^2}{E_a^2}R_a \quad (5)$$

and $\delta_{f\text{-}p}$ is assumed to be $\delta_{f\text{-}p}=54\delta_y$ [12,15].

Assuming further that the heights of pad asperities are exponentially distributed [16], the probability density function of asperity heights, $\phi(z_a)$, can be written as

$$\phi(z_a)=\frac{1}{\sigma_z}\exp\left(-\frac{z_a}{\sigma_z}\right) \quad (6)$$

As n asperities per unit nominal contact area are pressed against a smooth, flat surface layer, only the asperities taller than the separation distance, d, will be in contact. The ratio of real contact area to nominal contact area, A_r/A_n, between the pad and layer surfaces is the sum (or the integral) of individual asperity contributions. Thus

$$\frac{A_r}{A_n}=n\int_d^\infty A_a\phi(z_a)dz_a \quad (7)$$

For a given separation distance d, from Eqs. (3) and (6), and introducing $\xi=(z_a-d)/\sigma_z$, the contact area ratio can be expressed as

$$\frac{A_r}{A_n}=\pi R_a\sigma_z n\exp\left(-\frac{d}{\sigma_z}\right)f_A(\psi) \quad (8)$$

where f_A is a function of ψ:

$$\begin{aligned}f_A(\psi)=&\int_0^{1/\psi^2}\xi\exp(-\xi)d\xi\\ &+\int_{1/\psi^2}^{54/\psi^2}\left[1+3\left(\frac{\psi^2\xi-1}{53}\right)^2-2\left(\frac{\psi^2\xi-1}{53}\right)^3\right]\xi\exp(-\xi)d\xi\\ &+2\int_{54/\psi^2}^{\infty}\xi\exp(-\xi)d\xi\end{aligned} \quad (9)$$

and ψ is the plasticity index, defined as

$$\psi\equiv\left(\frac{\sigma_z}{\delta_y}\right)^{1/2}=\frac{4}{\pi}\frac{E_a}{H_a}\left(\frac{\sigma_z}{R_a}\right)^{1/2} \quad (10)$$

Similarly, from Eqs. (4), (6), and (10), the relation between the applied pressure, p, and the separation distance, d, can be estimated as

$$p=n\int_d^\infty p_aA_a\phi(z_a)dz_a=\pi H_aR_a\sigma_z n\exp\left(-\frac{d}{\sigma_z}\right)f_p(\psi) \quad (11)$$

where f_p is a function of ψ:

$$\begin{aligned}f_P(\psi)=&\frac{\psi}{3}\int_0^{1/\psi^2}\xi^{3/2}\exp(-\xi)d\xi\\ &+\int_{1/\psi^2}^{54/\psi^2}\frac{1}{3}\left[1+\frac{1}{2}\ln\psi^2\xi\right]\\ &\times\left[1+3\left(\frac{\psi^2\xi-1}{53}\right)^2-2\left(\frac{\psi^2\xi-1}{53}\right)^3\right]\xi\exp(-\xi)d\xi\\ &+2\int_{54/\psi^2}^{\infty}\xi\exp(-\xi)d\xi\end{aligned} \quad (12)$$

From Eqs. (8) and (11), the contact area ratio for a given nominal pressure, p, can be given as

$$\frac{A_r}{A_n}=\frac{p}{H_a}\frac{f_A(\psi)}{f_P(\psi)} \quad (13)$$

which indicates that the contact area ratio depends on the plasticity index, ψ, in addition to the normalized nominal pressure, p/H_a.

The plasticity index was first introduced by Greenwood and Williamson combining the topographical and mechanical properties of surfaces [17]. This dimensionless parameter characterizes the relative proportion of plastically deformed asperities in contact: higher plasticity index indicates greater proportion of plastic asperity contacts. Only when the index is much less than unity, can all asperities be assumed to deform elastically. If $\psi \ll 1$, Eq. (13) simplifies to

$$\frac{A_r}{A_n}=\sqrt{\pi}\frac{p}{E_a}\left(\frac{R_a}{\sigma_z}\right)^{1/2} \quad (14)$$

which is the Greenwood-Williamson model. For such elasticity-dominant contact, Young's modulus of asperities governs the mechanical behavior of asperity deformation. On the other hand, if $\psi \gg 1$, the equation simplifies to

$$\frac{A_r}{A_n}=\frac{p}{H_a} \quad (15)$$

which is the case of fully-plastic deformation. For such plasticity-dominant contact, the real contact area is determined by the asperity hardness and by the applied pressure. If ψ is near unity, which is the case of typical CMP pads [10], however, the asperity contacts comprise both elastically and plastically deformed asperities. Fig. 2 shows the contact area ratio versus the normalized pressure, p/H_a,

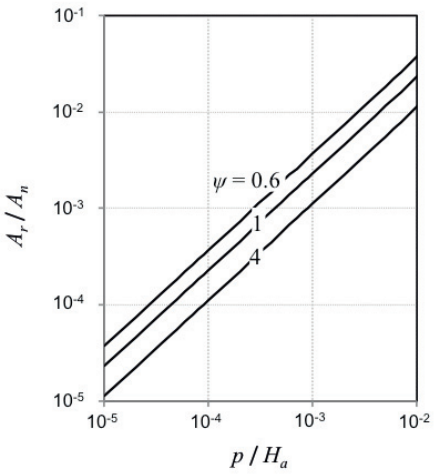

Fig. 2. Estimated contact area ratio, A_r / A_n, versus normalized pressure, p / H_a, for different plasticity indices, ψ.

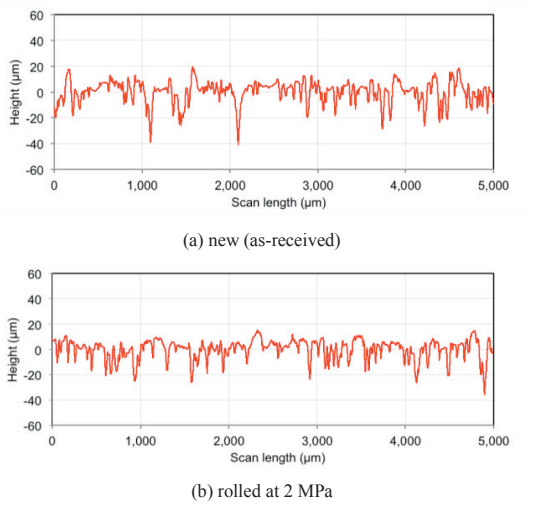

Fig. 3. Surface profiles of new and asperity-flattened IC1000 pads.

for different plasticity indices, ψ. Therefore, Eq. (2) is consistent with the Preston equation, Eq. (1), as the contact area ratio is proportional to the applied pressure and as the removal rate per particle is proportional to the relative velocity. Material removal rate, accordingly, will increase if the contact area ratio between the pad and wafer increases.

3. Pad topography control by asperity-flattening

The area ratio of rough pads in contact with flat wafer surfaces can be increased by applying higher pressure, or by using softer pads. In addition, the real contact area can also be increased by decreasing ψ, Eq. (10): i.e., either by increasing H_a/E_a or by increasing R_a/σ_z. The Young's modulus and the hardness of pad asperities, E_a and H_a, are difficult to change independently, whereas the topographical parameters, R_a and σ_z, are relatively easy to control. Recently, a simple process was introduced to increase R_a/σ_z i.e., by flattening the asperities using a smooth, flat plate or a smooth roller [10,11]. By pressing a flat metal plate at high pressure or by rolling/sliding a smooth metal roller, the radius of the tall asperities can be increased and the height variance reduced, thus increasing the value of R_a/σ_z. Although flattening requires much higher pressure (0.1 - 5 MPa) than the polishing pressure (10 - 50 kPa) typical pads, which have asperity hardness of about 100 MPa, will still contact but a few percent or less than the nominal contact area during flattening, Fig. 2. Therefore, only a few tall asperities will be flattened. It may be noted, however, that the compressed asperities may not be flat since flattened asperities may spring back partially by elastic recovery [18].

Asperities of circular disks, 20 mm in diameter, of the IC1000 pad were flattened by sliding a stainless steel cylinder, 4.8 mm in diameter, over the specimens at an average pressure of 2.3 MPa. The topographical properties, R_a and σ_z, and their ratio of new and flattened IC1000 pads, were determined from surface profiles obtained by a stylus profilometer, Fig. 3, and listed in Table 1. Then, by Eq. (13), the contact area ratios for the pads with different R_a/σ_z were estimated. A modulus-to-hardness ratio of 7.6 was used to estimate the plasticity indices. For selected applied pressures and constant mechanical properties of the pad, the real contact area increases as R_a/σ_z increases, Fig. 4, and therefore MRR is expected to be greater.

Table 1. Asperity radius, standard deviation of asperity heights, their ratio, and plasticity index of new and asperity-flattened IC1000 pads. All values are in μm.

Parameters	New (as-received)	Asperity-flattened
R_a (μm)	23.5	72.7
σ_z (μm)	4.4	3.3
R_a / σ_z	5.3	22.0
ψ	4.0	2.0

4. Polishing experiments and results

Cu-coated wafers were polished on a face-up polisher [10]. In experimental set 1, a slurry comprising 5 vol. % of Al_2O_3 abrasives of average size 300 nm was used. The polishing pressure was 13 kPa (2 psi) and the velocity was 0.87 m/s. In experimental set 2, a commercial slurry (HS-BT815, Hitachi Chemical Co.) was used. The pressure was 7 kPa (1 psi) and the velocity was 0.66 m/s. Table 2 lists the estimated contact area ratios from Eq. (13) and the results of the polishing experiments using new and asperity-flattened pads for the two different experimental conditions. The multi-asperity contact model predicts that the contact area ratio increases by about 37 and 36 percent, respectively. The polishing rates with the asperity-flattened pads indeed show 33 and 32 percent increase, respectively, compared with those using the new pads.

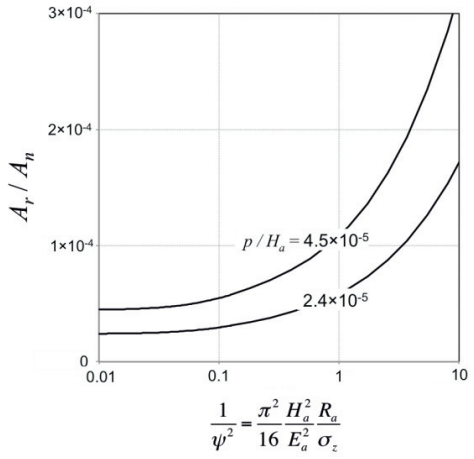

Fig. 4. Estimated contact area ratio, A_r / A_n, versus $1 / \psi^2$, when an IC1000 pad (E_a = 2.21 GPa, and H_a = 290 MPa) is pressed against a smooth, flat wafer surface at pressures p = 7 kPa (1psi) and 13 kPa (2 psi).

5. Discussion

Both the contact mechanics models and the experimental results show that MRR can be increased by increasing the R_a/σ_z; i.e., by increasing the asperity radius and/or by decreasing the standard deviation of asperity heights. Such results are due to the increase in real contact area at the pad/wafer interface. The benefit of the achieving the high R_a/σ_z value is that such pad topography not only improves MRR but also mitigates scratching. Pad scratching is due to the height variation of the asperities as the pressure will be concentrated on relatively tall asperities, which reach fully-plastic deformation. The high contact pressure and the interfacial friction at such asperities can be so large that even the soft pad asperities can generate scratches on relatively hard surfaces [9]. Accordingly, increasing R_a/σ_z of pad asperities can be effective in the mitigation of pad scratching by increasing the proportion of elastic contacts [10].

The "asperity-flattening" can effectively replace the current "breaking-in" process, producing fewer scratches at higher polishing rates and less usage of consumables. In order to reduce scratching in CMP, furthermore, the CMP practice adopts a method called "breaking-in". Before polishing wafers a new pad is "broken-in" by polishing about 50 Cu-coated wafers while continuously roughening the surface using a diamond conditioner. About one to four hours are required to break in a new pad. It was experimentally determined that as more Cu wafers are used, and thus longer the "break-in" is, MRR would be stable and scratching decreased [19,20]. Therefore, both time and expensive consumables, such as wafers and slurry, are wasted in the "breaking-in" process. The major reason why the industry accepts this inefficient process is the lack of clear understanding of the phenomenon of pad scratching. Table 3 shows the R_a/σ_z values of pad asperities after typical "breaking-in" process used in the semiconductor industry compared to those of new pads as received from pad manufacturer. The process indeed increases the R_a/σ_z, so that the "broken-in" pad can reduce scratching. However, since the process is not optimized for increasing R_a / σ_z, it is inefficient and expensive. Flattening the asperities, accordingly, by pressing a smooth, flat plate against, or by rolling/sliding a smooth roller over, the rough pad, accordingly, can be suggested as a alternative, inexpensive process to control the pad topography. Higher R_a/σ_z value can be achieved in much less process time, about 1 minute or less, compared with the current "break-in" process which in general takes one to four hours.

Table 2. Estimated contact area ratio, A_r / A_n, and the polishing rate of Cu layer, dh / dt, (polished by new and asperity-flattened pads). Experimental sets 1 and 2 used different slurry, nominal pressure and relative velocity.

Parameters	New (as-received)	Asperity-flattened	Percent increase
Experimental set 1			
A_r / A_n (estimated)	2.7×10^{-5}	3.7×10^{-5}	37
dh / dt (Å/min)	833	1110	33
Experimental set 2			
A_r / A_n (estimated)	5.0×10^{-5}	6.8×10^{-5}	36
dh / dt (Å/min)	690	909	32

Table 3. Asperity radius, standard deviation of asperity heights, their ratio, and the estimated plasticity indices of new and "broken-in" IC1000 pads.

Parameter	New pad	"Broken-in" pad
R_a (μm)	23.5	53.8
σ_z (μm)	4.4	3.2
R_a / σ_z	5.3	16.8
Ψ	4.0	2.4

A greater challenge in pad topography control, however, is the maintenance of the enhanced R_a/σ_z value through the pad life. During the polishing of wafers, the pad asperities are worn out by the hard abrasives in the slurry and thus the R_a/σ_z will also continuously change. Locating a loaded roller between the conditioner and the wafer, as in Fig. 5, can be introduced for in-situ flattening while polishing, although more investigation is required to be conceived and tested for practical implementation.

Concerns may arise on the "asperity-flattening" process, as the process can affect the average roughness of the pad surface. Reduction in average roughness is known to reduce MRR due to the constriction of slurry flow from the edge to the center of the wafer or due to the hydroplaning [21-24]. It may be noted, however, that although lower surface roughness of the pad might result in smaller standard deviation of asperity heights, large asperity radius does not necessarily require low surface roughness. A pad surface can have a high R_a / σ_z and high average roughness simultaneously by having large average radius and large average height but with small variance. Flattening the tall asperities by compression or by rolling/sliding, can achieve higher polishing rate by decreasing the plasticity index without much decreasing in average

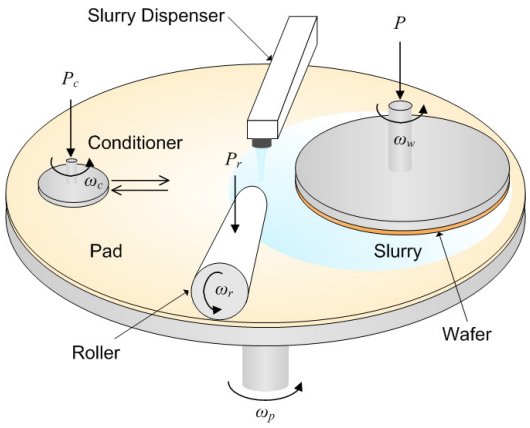

Fig. 5. Schematic of in-situ asperity flattening by a truncated conical roller.

roughness appreciably. Shown in Table 4 are the roughness parameters of new and asperity-flattened pads. Because only the tall asperities are flattened, the decrease in average roughness of the pad surface is less than ten percent, whereas the decrease in the maximum peak height is over 30 percent.

Table 4. Surface roughness of new and asperity-flattened IC1000 pads. All values are in μm.

Parameters	New (as-received)	Asperity-flattened
Ra (arithmetic average)	6.18	5.52
Rq (root mean square)	8.24	7.24
Rp (maximum peak height)	22.72	15.50
Rv (maximum valley depth)	31.05	30.81
Rt (=Rp – Rv)	53.78	46.30

6. Conclusion

In this study, the effects of pad topography on the material removal rate in CMP have been investigated. Contact mechanics models predict that the material removal rate can be improved by increasing the ratio of asperity radius and the standard deviation of asperity heights, R_a/σ_z. which results in an increase in real area of contact. Asperity-flattening process significantly enhances the R_a/σ_z while not reducing the average roughness appreciably. Cu polishing experiments using asperity-flattening process indeed showed an increase in polishing rate by about 30 percent, which agrees with theoretical predictions. Further improvements in MRR can be achieved by optimizing the asperity-flattening process.

Acknowledgments

The present study was funded by the Samsung Electronics Company, Ltd.

References

[1] Zantye PB, Kumar A, Sikder AK. Chemical mechanical planarization for micro electronics applications. Mater Sci Eng R 2004; 45: 89-220.
[2] Preston FW. The theory and design of plate glass polishing machines. J Soc Glass Tech 1927; 11: 214-256.
[3] Paul E. A model of chemical mechanical polishing. J Electrochem Soc 2001; 148(6): G355-G358.
[4] Luo J, Dornfeld DA. Material removal mechanism in chemical mechanical polishing: theory and modelling. IEEE Trans Semicon Manuf 2001; 14(2): 112-133.
[5] Zhao Y, Chang L. A micro-contact and wear model for chemical-mechanical polishing of silicon wafers. Wear 2002; 252: 220-226.
[6] Chandrasekaran N, Ramarajan S, Lee W, Sabde M, Meikle S. Effects of CMP process conditions on defect generation in low-*k* materials. J Electrochem Soc 2004; 151(12): G882-G889.
[7] Chandra A, Karra P, Bastawros AF, Biswas R, Sherman PJ, Armini S, Lucca DA. Prediction of scratch generation in chemical mechanical planarization. Annals of the CIRP 2008; 57(1): 559-562.
[8] Saka N, Eusner T, Chun J-H. Nano-scale scratching in chemical-mechanical polishing. Annals of the CIRP 2008; 57(1): 341-344.
[9] Saka N, Eusner T Chun J-H. Scratching by pad asperities in chemical-mechanical polishing. Annals of the CIRP 2010; 59: 329-332.
[10] Kim S, Saka N, Chun J-H, Shin S-H. Modeling and mitigation of pad scratching in chemical-mechanical polishing, Annals of the CIRP 2013; 62: 307-310.
[11] Saka N, Chun J-H, Kim S, Shin S-H. Scratch reduction by pad topography control in chemical-mechanical polishing. US Provisional Patent 2013; Application number: 61/758,449.
[12] Choi S, Doyle FM, Dornfeld D. A model of material removal and post process surface topography for copper CMP. Procedia Engineering 2012; 19: 73-80.
[13] Zhao Y, Maietta DM, Chang L. An asperity microcontact model incorporating the transition from elastic deformation to fully plastic flow. ASME J Tribol 2000; 122(1): 86-93.
[14] McCool JI. Comparison of models for the contact of rough surfaces, Wear 1986; 107: 37-60.
[15] Johnson KL. Contact Mechanics. Cambridge University Press. Cambridge UK; 1985.
[16] Vasilev B, Bott S, Rzehak R, Liske R, Bartha JW. A method for characterizing the pad surface texture and modeling its impact on the planarization in CMP. Microelectronic Eng 2013; 104: 48-57.
[17] Greenwood JA, Williamson JBP. Contact of nominally flat surfaces. Proc Roy Soc Lond A 1966; 295: 300-319.
[18] Kadin Y, Kligerman Y, Etsion I. Unloading an elastic-plastic contact of rough surfaces. J Mech Phys Solids 2006; 54: 2652-2674.
[19] Luo Q, Ramarajan S, Babu SV. Modification of the preston equation for the chemical-mechanical polishing of copper. Thin Solid Films 1998; 335: 160-167.
[20] Eusner T, Saka N, Chun J-H. Breaking-in a pad for scratch-free, Cu chemical-mechanical polishing. J Electrochem Soc 2011; 158(4): H379-H389.
[21] McGrath J, Davis C. Polishing pad surface characterization in chemical mechanical planarization. J Mater Process Tech 2004; 153-154: 666-673.
[22] Lee H, Zhuang Y, Sugiyama M, Seike Y, Takaoka M, Miyachi K, Nishiguchi T, Kojima H, Philipossian A. Pad flattening ratio, coefficient of friction and removal rate analysis during silicon dioxide chemical mechanical planarization. Thin Solid Films 2010; 518: 1994-2000.
[23] Shi H, Ring TA, CMP pad wear and polish-decay modeled by asperity population balance with fluid effect. Microelectronic Eng 2010; 87: 2368-2375.
[24] Hooper BJ, Byrne G, Galligan S. Pad conditioning in chemical mechanical polishing. J Mater Process Tech 2002; 123: 107-113.